72435

Micropoikilitic Impact Melt Breccia
St. 2, 160.6g

INTRODUCTION

72435 is a very fine-grained, clast-bearing impact melt with a micropoikilitic texture. It was sampled as typical matrix of Boulder 3, Station 2 (see section on Boulder 3, Station 2, Fig. 1). The sample has a major and trace element chemistry similar to other Apollo 171ow-K Fra Mauro impact melts, and can be assumed to have formed in the Serenitatis event. It is among the finest-grained of such samples. Radiogenic isotopic data on matrix and clasts show that it crystallized close to 3.86 Ga ago, and that matrix and clasts did-not totally equilibrate with each other, even for argon. The larger clasts are dominantly feldspathic granulites, and brecciated dunitic, troctolitic, and noritic fragments.

The sample, consisting of two mated pieces (4 x 5 x 3 cm, and 5 x 4 x 3 cm) is angular, and gray (N4) (Fig. 1). It is commonly referred to as blue-gray (e.g. LSPET, 1973). It is tough but with one penetrative fracture that broke the sample. The sample is-homogeneous, except for apparent variation in grain size near some cavities. Clasts up to 1 cm are visible in the sample; larger clasts (including the sampled dunite) were visible in the parent boulder. Clasts larger than 1 mm compose about 5% of the sample. Both clasts and elongate cavities in 72435 are aligned, but most cavities are spherical. Some are as large as 8 mm. Smaller cavities are smooth or drusy; some larger ones have crystal linings. Cavities occupy less than 1 % of the sample. The exposed surface (B and W) are knobby, discolored, and rounded, with zap pits. The broken interior is hackly.

Most of the studies of 72395 were conducted under a consortium led by the Caltech group (Dymek et al., 1976a; Papanastassiou and Wasserburg 1975a; Huneke, 1978). Following chipping of two small samples, advantage was taken of the samples breakage to produce a slab with a single saw cut across the large of the ends. This slab was dissected (Fig. 2), and nearly all subsequent allocations were made from this slab.

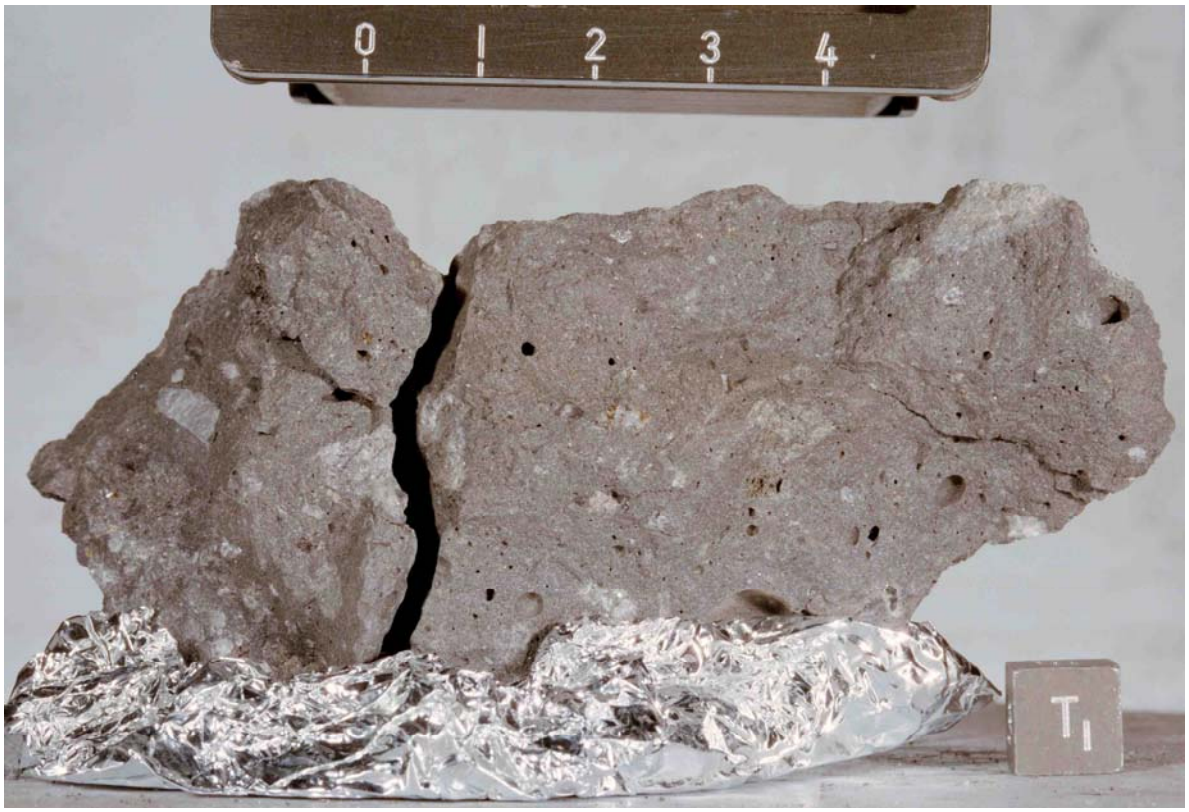

Figure 1: Fractured surface of 72435. Clasts as large as 10 mm are visible, as well as vesicles up to 8 mm (lower center right). Scale in centimeters. S-73-19652.

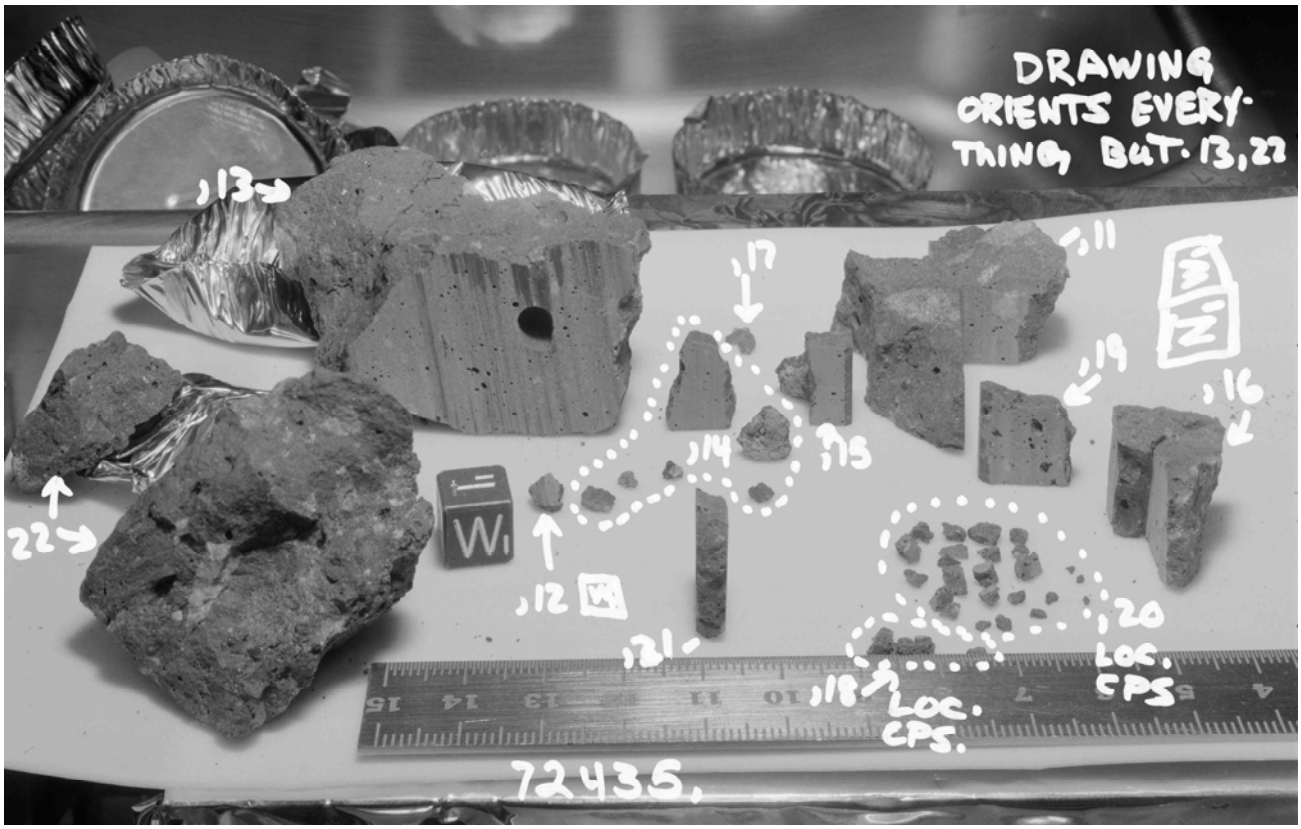

Figure 2: Dissection of 72435 with a single saw-cut across the larger end. Cube is 1 cm across. S-74-23143.

PETROGRAPHY

72435 consists of mineral and lithic clasts in an extremely fine-grained, poikilitic, partially elastic matrix (Dymek et al., 1976a, b). The sample formed as the result of crystallization of a clast-bearing melt produced in an impact. In thin section the matrix has a dark gray appearance resulting from the aphanitic nature (Fig. 3a). The larger clasts are lithic fragments, most less than 2 cm across. The smaller clasts include abundant mineral clasts. According to Dymek et al. (1976a), clasts in the 1 to 20 mm range compose 5 to 10% of the sample. The igneous groundmass has an average grain-size of less than 50 microns (Fig. 3b), and the microclasts have a seriate grain-size distribution. Simonds et al. (1974) referred to 72435 as a crystalline, matrix-supported, micropoikilitic rock with matrix feldspars 5 to 30 microns long and matrix mafic grains 25 to 50 microns long. Chao and Minkin (1974b) noted that 72435 was similar to 77135. Albee et al. (1974) noted that the sample differs from the Boulder 2, Station 2 samples in being blue-gray, having fewer and smaller clasts, and some larger vesicles; they also noted some zones of aligned slit vesicles.

The most detailed petrographic description of both clasts and matrix for 72435 are by Dymek et al. (1976a), who present microprobe data. Further details on a specific spinet-troctolite clast were given by Herzberg (1978), Herzberg and Baker (1980), and Baker and Herzberg (1980a,b). Most of the groundmass is homogeneous, but there are some areas (about 300 microns) that are much finer-grained. Other areas up to 500 microns across contain aggregates of plagioclase laths; these might be either clasts or a type of "synneusis" texture. The groundmass appears to be unaffected by the local alignment of slit vesicles and clasts. Dymek et al. (1976a) listed the phase abundances, phase compositions, and the bulk chemical composition (from a microprobe point count) of 72435 (Table 1). The tabulated phase compositions appear to represent those of the groundmass, not clasts. These authors also diagrammed the mineral compositions for the sample, reproduced here as Fig. 4 (plagioclases), Fig. 5 (pyroxenes), Fig. 6 (olivines and Fe-Ti oxides), Fig. 7 (spinels), and Fig. 8 (metal). Most of these diagrams include data from dunite 72415-7 for comparison, and distinguish clasts from groundmass phases.

The groundmass consists of fine-grained intergrown pyroxene, plagioclase, olivine, and ilmenite. The mafic silicate grains form tiny oikocrysts (about 10-50 microns across) that enclose tinier grains of plagioclase; most of the ilmenite is interstitial to the oikocrysts (Fig. 3b). Most of the oikocrysts are low-

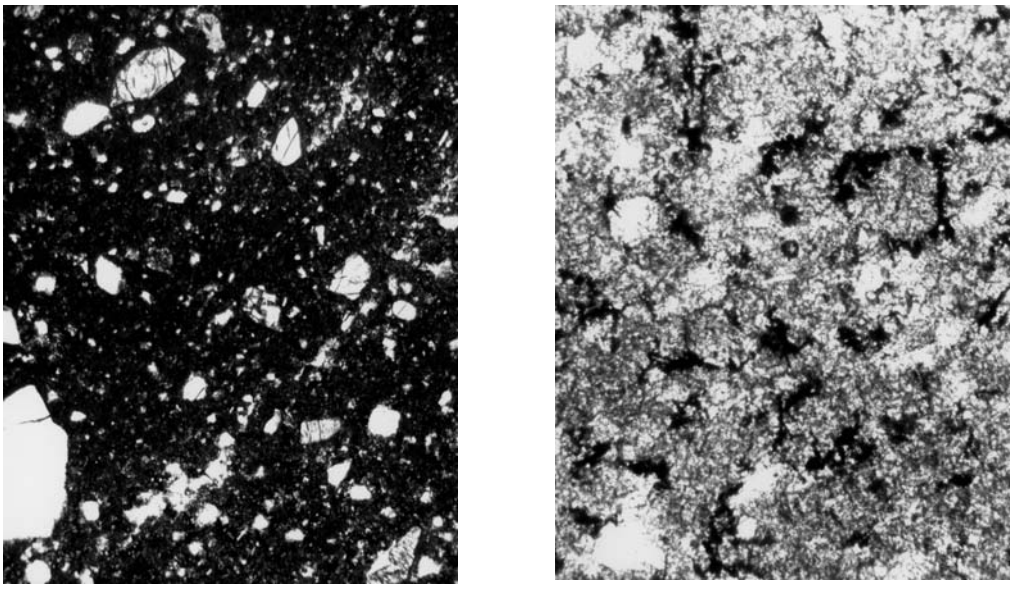

a b

Figure 3: Photomicrographs of 72435, 7. Both transmitted light, fields of view about 1 mm (a) and about 300 microns (b). a) shows the dense nature of the groundmass, the subrounded/subangular nature of the clasts, and the small size of most clasts. b) shows the igneous nature of the groundmass, with ilmenite (black) forming interstitially to the mafic oikocrysts, which seem mottled because they are studded with tiny plagioclases.

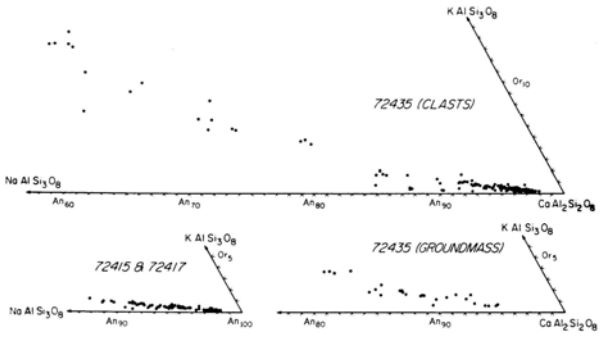

Figure 4: Compositions of plagioclases in 72435, with groundmass and clast plagioclases distinguished, and data for dunite 72415-7 for comparison (Dymek et al., 1976a).

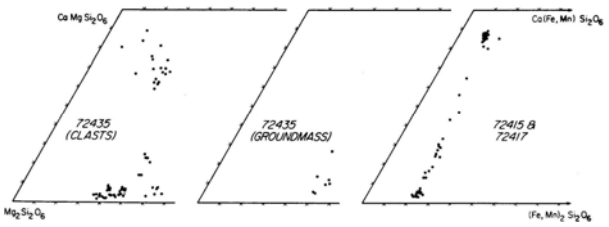

Figure 5: Compositions of pyroxenes in 72435, with groundmass and clast pyroxenes(distinguished, and data for dunite 72415-7 for comparison (Dymek et al., 1976a).

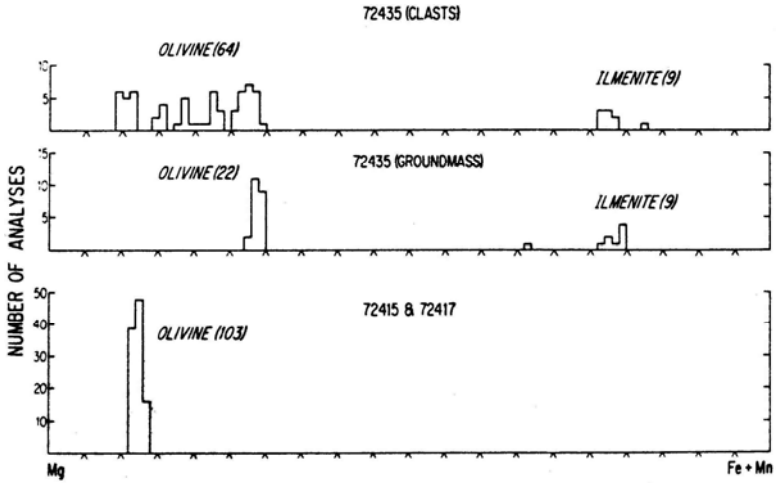

Figure 6: Compositions of olivines in 72435, with groundmass and clast olivines distinguished and data for dunite 72415-7 for comparison (Dymek et al., 1976a).

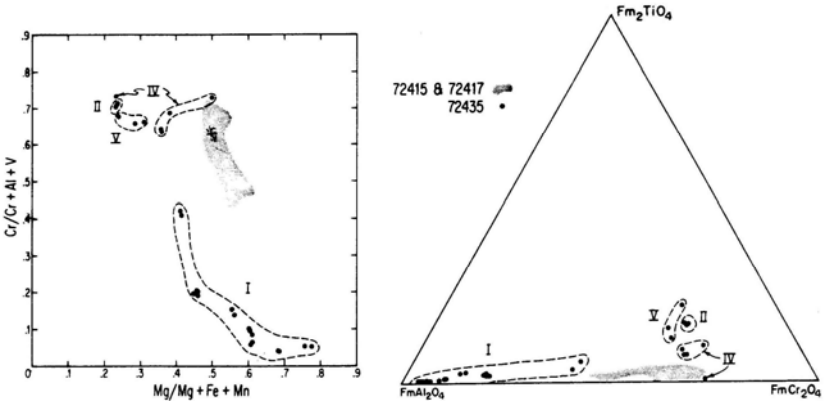

Figure 7: Compositions of spinets in 72435, with groundmass and clast spinels distinguished, and data for dunite 72415-7 for comparison (Dymek et al., 1976a).

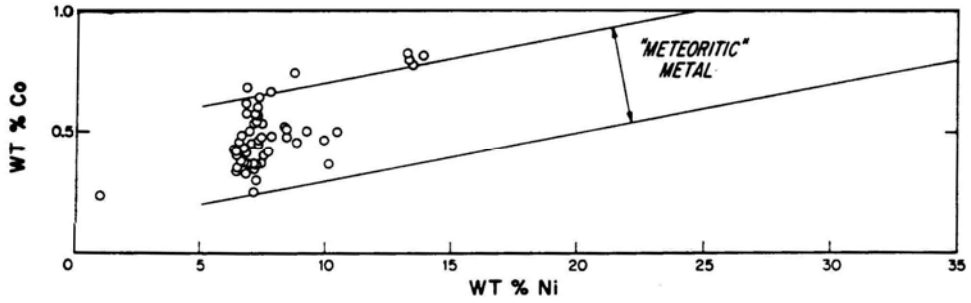

Figure 8: Ni and Co concentrations of metals in 72435 groundmass. Most fall in the "meteoritic" field. (Dymek et al., 1976a).

Table 1: Phase abundances, "average" phase compositions, and calculated bulk chemical composition of 72435,39. (Dymek et al., 1976a).

	Plag.	Low-Ca pyx	High-Ca pyx	Olivine	Ilmenite	Troilite*	Metal*	Ca-Phos.†	Meso-stasis	SiO_2	Bulk comp.
Vol.%	63.0	21.0	3.8	8.1	1.9	0.0	0.1	0.3	0.9	0.6	
±1 σ	2.8	1.6	0.7	1.0	0.5	0.0	0.1	0.1	0.3	0.2	Calculated
Wt.%	57.5	23.9	4.2	9.5	2.7	0.0	0.3	0.3	0.7	0.5	(777 points)
P_2O_5	n.a.	n.a.	n.a.	n.a.	n.a.	n.a.	n.a.	43.15	0.09	n.a.	0.15
SiO_2	45.46	52.77	51.96	37.71	0.31	<0.1	<0.01	—	64.10	99.93	45.59
TiO_2	0.09	1.03	1.85	0.10	53.53	n.a.	<0.01	—	1.92	<0.01	1.85
Al_2O_3	34.98	1.39	2.53	<0.01	0.08	n.a.	n.a.	—	16.79	0.48	20.71
Cr_2O_3	n.a.	0.40	0.67	0.10	0.40	n.a.	n.a.	—	<0.01	n.a.	0.14
MgO	0.07	25.33	17.38	36.65	5.98	n.a.	<0.01	—	0.11	0.03	10.49
FeO	0.12	14.87	8.01	26.12	39.12	63.12	91.26	—	1.19	0.04	8.01
MnO	n.a.	0.20	0.19	0.21	0.39	0.05	n.a.	—	0.01	n.a.	0.09
CaO	18.48	3.83	17.88	0.11	n.a.	n.a.	n.a.	54.54	1.28	0.03	12.51
Na_2O	1.12	0.02	0.13	n.a.	n.a.	n.a.	n.a.	—	0.26	<0.01	0.66
K_2O	0.21	n.a.	n.a.	n.a.	n.a.	n.a.	n.a.	—	13.31	0.25	0.23
BaO	0.11	n.a.	n.a.	n.a.	n.a.	n.a.	n.a.	—	1.29	0.24	0.07
ZrO_2	n.a.	n.a.	n.a.	n.a.	<0.01	n.a.	n.a.	—	<0.01	n.a.	<0.01
V_2O_3	n.a.	n.a.	n.a.	n.a.	<0.01	n.a.	n.a.	—	n.a.	n.a.	<0.01
Nb_2O_5	n.a.	n.a.	n.a.	n.a.	0.19	n.a.	n.a.	—	n.a.	n.a.	<0.01
NiO	n.a.	n.a.	n.a.	<0.01	n.a.	<0.01	7.18	—	n.a.	n.a.	0.03
Co	n.a.	n.a.	n.a.	n.a.	n.a.	<0.01	0.58	—	n.a.	n.a.	<0.01
S	n.a.	n.a.	n.a.	n.a.	n.a.	37.25	<0.01	—	n.a.	n.a.	0.03
F	n.a.	n.a.	n.a.	n.a.	n.a.	n.a.	n.a.	2.31	n.a.	n.a.	<0.01
Total	100.63	99.85	100.61	101.01	100.00	100.42	99.02	100.00	100.37	101.01	
	An 89.0	Wo 5.6	Wo 32.4	Fo 71.3							
	Ab 9.8	En 67.8	En 47.9	Fa 28.7							
	Or 1.2	Fs 22.6	Fs 12.7								
	Others	4.0	7.0								

*Elemental abundances; converted to oxides for calculating bulk composition.
†Assumed 1:1 mixture of fluorapatite and whitlockite.
n.a. = Not analyzed.

Ca pyroxenes ($En_{73}Wo_2$ to $En_{62}W0_{14}$); some are high-Ca pyroxenes, and others are olivines (Fo_{72-70}). Olivine also occurs at oikocryst boundaries. Most of the plagioclase chadacrysts form euhedral laths less than 10 microns across, and compose up to a third of the area of the oikocryst. Orientations are random. Most chadacrysts are An_{91-85}; laths outside the oikocrysts range from An_{95-80}. Ilmenite occurs interstitially as bladed grains 1-10 microns wide, and as tiny blebs, some of which are in oikocrysts. The groundmass also contains interstitial troilite, Fe-metal, and areas of K-rich mesostasis with small phosphate grains.

Most of the clasts are single mineral fragments, and include plagioclase, olivine, low- Ca pyroxenes, and much less common high-Ca pyroxene, metal, ilmenite, and spinet. Variation in size, angularity, degree of shock, and composition indicate a variety of sources. They tend to have wider ranges in composition than groundmass phases. Plagioclases include untwinned and twinned types, ranging from subrounded to subangular, and from subequant to elongate. They vary from unshocked and clear, to shocked with cloudy or undulose extinction features, including feathery/spherulitic aggregates. Zoning is only rarely present. The range in compositions is extremely large ($An_{55}Ab_{30}Or_{15}$ to $An_{98}Ab_{2O}r<1$), and includes compositions both less refractory and more refractory than groundmass plagioclases. Some have reaction rims; rarely plagioclases clasts are extensively resorbed. Most pyroxenes are subequant. They range from very pale green and brown to darker, mottled fragments that are probably shocked. Most are homogeneous in composition, and are at least as magnesian as groundmass grains. Olivines ($F0_{92-70}$) range from strain-free, virtually colorless grains to those with abundant strain bands and partings. Some are zoned; reaction rims are not present, and edge compositions are equivalent to groundmass olivines. Spinet clasts have spectacular reaction rims.

Most of the lithic clasts in 72435 are feldspathic highlands lithologies, similar to those in Boulder 2, Station 2 samples, and compose several percent of the rock. They have a range of textures, grain sizes, and compositions. Plagioclases in these fragments are generally more calcic than An_{90}, Pyroxenes and olivines have compositions similar to those of the mineral clasts. The lithologies (according to Dymek et al., 1976a) include recrystallized anorthositic, noritic, and troctolitic rocks, poikilitic norites, dunites, and spinet cataclasite. Many of these are feldspathic granulitic breccias, i.e. recrystallized. The dunites resemble 72415-8 samples i.e., coarse-grained. Some fine-grained samples differ in having polygonal textures and are not cataclasites.

Dymek et al. (1976a) noted two spinet cataclasite fragments, a distinctive lithology, and reported mineral analyses. The fragments are friable, and consist of a broken

assemblage of plagioclase (70%; An_{98-94}), olivine (20%; Fo_{72}), pink spinet (5%), low-Ca pyroxene (1%), and smaller amounts ilmenite, troilite, and Fe-metal. One of the clasts contains a single grain of cordierite (30 microns) as an inclusion in spinet. No high-Ca pyroxene was observed by Dymek et al. (1976a). The major mineral phases are unshocked and clear. Herzberg (1978), Herzberg and Baker (1980), and Baker and Herzberg (1980a b) further studied the spinet cataclasites in an attempt to define temperatures and pressures of origin from thermodynamic constraints based on experimental data. They provided new mineral composition data (Figs. 9, 10) that is consistent with the Dymek et al. (1976a) data and detailed petrographic descriptions. A summary of the compositions and conclusions based on them is given as Table 2, with the cordierite-bearing (in ,8) and cordierite-free (in ,30) samples distinguished. Ranges in composition of spinets and pyroxenes show that the fragments are not in equilibrium, and some grains may not be indigenous. However, much of the olivine, spinet, and pyroxene may be in equilibrium. The two samples produce different estimates of the pressure, with the cordierite-free sample suggestive of mid- to lower-crust levels, and the cordierite bearing sample giving negative pressures.

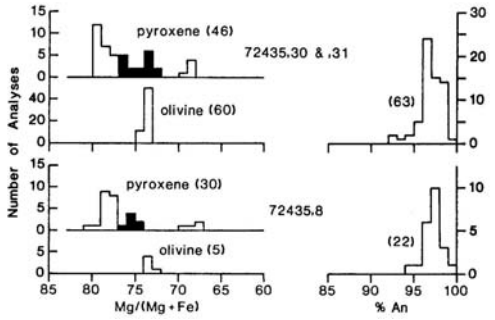

Figure 9: Summary of compositions of low-Ca pyroxene, olivine, and plagioclase in 72435 spinel cataclasites. Number of analyses in parentheses. The compositional range of pyroxenes in apparent equilibrium with coexisting olivine in each field is shaded. 72435,8 is cordierite bearing; the others are cordierite-free. (Baker and Herzberg, 1980a).

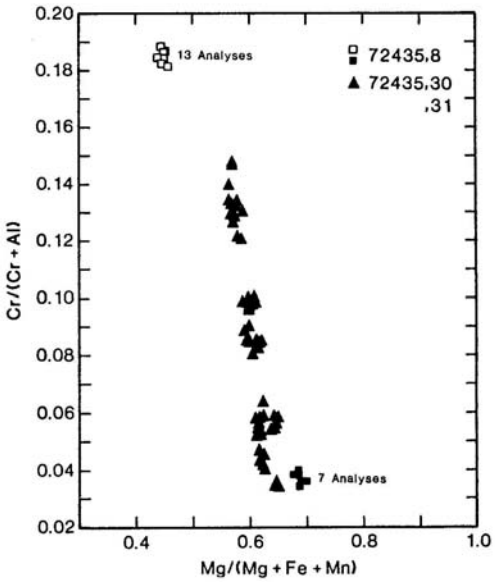

Figure 10. Compositions of spinels in 72435 spinel cataclasites. 72435,8 is cordierite-bearingl; the others are cordierite-free. (Baker and Herzberg, 1980a).

CHEMISTRY

Chemical analyses of bulk rock (groundmass plus clasts) for 72435 are given in Table 3; the major element analyses agree fairly well with that derived by Dymek et al. (1976a) from a microprobe point count (Table 1). The rare earth elements are plotted as Figure 11. These data were reported with little specific discussion. The sample has a low-K Fra Mauro basalt composition, similar in major and trace elements to many other impact melt samples at the Apollo 17 site. It clearly has meteoritic contamination, but the siderophile element data are inadequate to specify a meteoritic group (a la Anders group)

RADIOGENIC ISOTOPES AND GEOCHRONOLOGY

Rubidium and strontium isotopic data for whole-rock samples of 72435 were reported by Nyquist et al. (1974a, b) and Papanastassiou and Wasserburg (1975a, b), and the latter authors also reported data for splits derived from handpicking of clasts and density separations of a matrix sample. These isotopic data are reproduced in Tables 4 (whole rock) and 5 (separates).

According to Nyquist et al. (1974a), the data lie on a line with other Apollo 17 melt samples with a slope equivalent to an age of 3.94 +1-0.1 Ga. 72435 has lower Rb than most of these other samples, giving older model ages. Papanastassiou and Wasserburg (1975a) found that

Table 2: Pressure-temperature summary for spinel cataclasites in 72435, with summary of relevant mineral compositions. (Baker and Herzberg, 1980a).

72435,30

Olivine (Fo_{73}), Orthopyroxene [Mg/(Mg + Fe) = 0.78, Al_2O_3 = 3.83 wt %, Ti/Al = .14], Spinel [Mg/(Mg + Fe) = 0.57 − 0.64, Al/(Al + Cr) = .87 − .94], Plagioclase (An_{96})

Selenothermometer	T(°C)	Depth (km) I	Depth (km) II
1	1000–1200	≥32	≥12
2	800–1200	≥28	≥12
3	680– 810	≥26	≥12
4	1170–1230	≥32	≥12

I: from highest Al/(Al + Cr) and Mg/(Mg + Fe) in spinel
II: from lowest Al/(Al + Cr) and Mg/(Mg + Fe) in spinel

72435,8

Olivine (Fo_{73}), Orthopyroxene [Mg/(Mg + Fe) = .75, Al_2O_3 ≃ 4 wt %, Ti/Al ≃ 0.11], Cordierite [Mg/(Mg + Fe) = .84], Spinel [Mg/(Mg + Fe) = .45, Al/(Al + Cr) = 0.81], Plagioclase (An_{97}).

Selenothermometer	T(°C)	Depth (km)* I	Depth (km)* II
1	700	−6	−12
2	no solution	?	
3	950–1020	−10	−18
4	1290–1310	−16	−24

* 72435,8 is a univariant mineral assemblage. In principle, a specific T and P can be determined.
I: from lowest Al_2O_3 in opx
II: from highest Al_2O_3 in opx

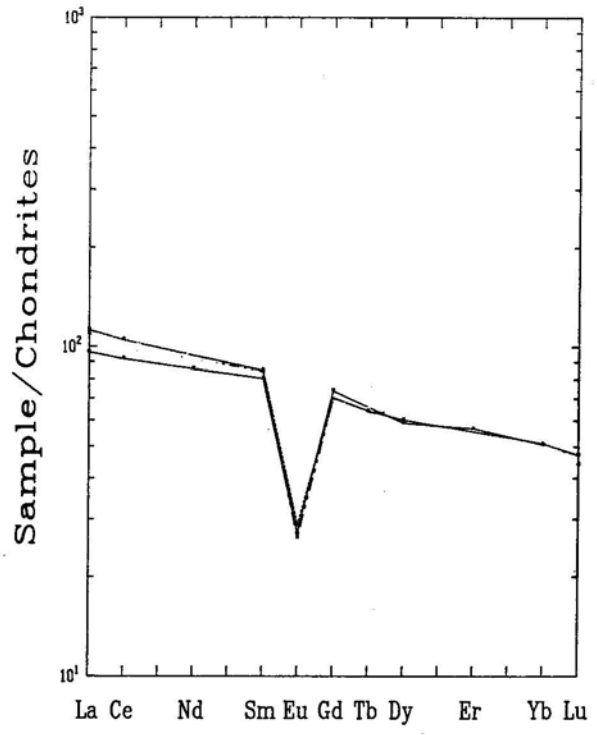

Figure 11: Rare earth elements in splits of 72435. Solid line is, 1 (Hubbard et al., 1974; Nyquist et al., 1974a). Fine dashed line is ,11 (Murals et al., 1977)

Table 3: Chemical analyses of bulk rock for 72435.

Split	,1	,1	,11	,1	,11 T-1	,11 T-2	,11 (a)	Split
wt %								wt %
SiO_2	45.76							SiO_2
TiO_2	1.54		1.5					TiO_2
Al_2O_3	19.23		17.8					Al_2O_3
Cr_2O_3	0.20	0.1185	0.217					Cr_2O_3
FeO	8.70		10.4					FeO
MnO	0.11		0.112					MnO
MgO	11.63		12					MgO
CaO	11.72		10.4					CaO
Na_2O	0.52		0.67					Na_2O
K_2O	0.23	0.2163	0.23		0.2394	0.2393	0.2131	K_2O
P_2O_5	0.27							P_2O_5
ppm								ppm
Sc			17					Sc
V			50					V
Co			31					Co
Ni	112		320					Ni
Rb	3.8	3.93			3.528	3.445	2.762	Rb
Sr	165	171.6			168.0	169.5	165.4	Sr
Y	107							Y
Zr	450	473	430					Zr
Nb	30							Nb
Hf		12.7	11.5					Hf
Ba		334	310					Ba
Th			3.0					Th
U		1.40						U
Cs								Cs
Ta			1.9					Ta
Pb								Pb
La		31.7	37.0					La
Ce		80.6	92					Ce
Pr								Pr
Nd		51.3						Nd
Sm		14.5	15.3					Sm
Eu		1.88	1.98					Eu
Gd		18.3						Gd
Tb			3.0					Tb
Dy		18.6	19					Dy
Ho								Ho
Er		11.3						Er
Tm								Tm
Yb		10.1	10.2					Yb
Lu			1.6					Lu
Li		17.5						Li
Be								Be
B								B
C								C
N								N
S	800			945				S
F								F
Cl								Cl
Br								Br
Cu								Cu
Zn	2							Zn
ppb								ppb
Au			6					Au
Ir			9					Ir
	(1)	(2)	(3)	(4)	(5)	(5)	(5)	

References and methods.
1) LSPET (1973); XRF
2) Hubbard et al. (1974), Nyquist et al. (1974a); ID/Ms except Na by AAS
3) Murali et al. (1977); INAA
4) Gibson and Moore (1974a); combustion
5) Papanastassiou and Wasserburg (1975a); ID/MS

Notes
(a) matrix adjacent to clast E.

Table 4: Whole-rock Rb-Sr isotopic data for 72435. Ages have been recalculated for new decay constant for ^{87}Rb (decay constant =1.42 x 10-11 $^{y-1)}$ and are +/-.06 to .09 Ga. Isotopic ratios have not been adjusted for inter-laboratory bias.

Reference	Rb ppm	Sr ppm	$^{87}Rb/^{86}Sr$	$^{87}Sr/^{86}Sr$	T_{BABI}	T_{LUNI}
Nyquist et al. (1974a)	3.93	171.6	0.0662+/-6	0.70360+/-5	4.63	4.70
Papanastassiou and Wasserburg (1975a)	3.528	168.0	0.0609	0.70306+/-5	4.57	
	3.445	169.5	0.0589	0.70300+/-5	4.65	
	2.762	165.4	0.0484	0.70245+/-6	4.88	

Table 5: Rubidium and strontium isotopic data for 72435 whole-rock and separates as reported by Papanastassiou and Wasserburg (1975a). T_{BABI} ages are for a decay constant of 1.39 x 10^{-11} y^{-1}. The first two and the last rows appear in modified form in Table 4.

Sample[a]		Weight mg	K[f] ppm	Rb[f] 10^{-8} mole/g	^{88}Sr[f]	$^{87}Rb/^{86}Sr$ $\times 10^2$	$^{87}Sr/^{86}Sr$[g]	T_{BABI}(AE)
Total-1	M	73	1995	4.128	158.0	6.09	0.70306 ± 5	4.67 ± 0.06
Total-2	M	35	1944	4.031	159.5	5.89	0.70300 ± 5	4.75 ± 0.06
Total-clast A	M	21	755	2.819	126.1	5.21	0.70234 ± 5	4.50 ± 0.07
Plag clasts	M	3.4	776	0.879	242.3	0.846	0.69957 ± 4	—
Density separates (on 2.8 g of matrix)								
$2.70 < \rho < 2.80$	L	15	—	5.70	260.8	5.10	0.70240 ± 4	4.67 ± 0.05
$2.60 < \rho < 2.70$	L	5.3	7725	25.11	258.5	22.65	0.71318 ± 4	4.37 ± 0.02
		2.5[e]	7350	23.70	257.7	21.45	0.71245 ± 11	4.38 ± 0.04
$2.40 < \rho < 2.45$	L	1.9	2990	12.11	186.6	15.14	0.70828 ± 6	4.29 ± 0.03
		1.6[e]	2440	8.75	168.2	12.13	0.70657 ± 7	4.37 ± 0.04
$2.35 < \rho < 2.40$	L	2.3	2315	7.35	169.0	10.14	0.70540 ± 5	4.42 ± 0.03
Density separates (on 48 mg of matrix)								
$2.6 < \rho < 2.8$	L	2.2	2186	4.46	199.4	5.22	0.70250 ± 5	4.69 ± 0.07
$2.4 < \rho < 2.5$	L	1.6	1886	4.65	142.8	7.60	0.70396 ± 9	4.57 ± 0.08
$2.8 < \rho < 3.0$	L	2.3	2503	6.64	183.1	8.45	0.70448 ± 5	4.54 ± 0.02
Clast E								
Plag[b]-1	M	1.2	1148	2.141	174.2	2.867	0.70074 ± 6	—
-2	M	1.0	1464	2.575	178.2	3.370	0.70111 ± 9	—
-3	M	3.5	1725	4.495	197.3	5.32	0.70206 ± 7	—
-4	M	4	1740	5.067	203.1	5.82	0.70239 ± 4	4.10 ± 0.05
-5	M	1.6	1584	4.948	180.1	6.41	0.70271 ± 8	4.07 ± 0.09
Rim[c]-1	M	2.3	2006	3.893	198.5	4.57	0.70199 ± 9	4.59 ± 0.14
-2	M	1.6	2043	4.076	178.7	5.32	0.70246 ± 7	4.56 ± 0.09
-3	M	0.8	1930	4.374	174.8	5.84	0.70270 ± 12	4.44 ± 0.14
Matrix[d]-1	M	3.9	1776	3.232	155.6	4.84	0.70245 ± 6	4.98 ± 0.09

[a]Sample obtained mechanically [M] or by heavy liquid density separations [L].
[b]Samples from the interior of the clast.
[c]Samples from pink-grey rim of clast.
[d]Matrix sample adjacent to clast E.
[e]Repeat analysis.
[f]Uncertainties in the concentrations: K ± 1%; Rb ± 0.4%; ^{88}Sr ± 0.1%.
[g]Uncertainties correspond to last significant figures and are $\pm 2\sigma_{mean}$.

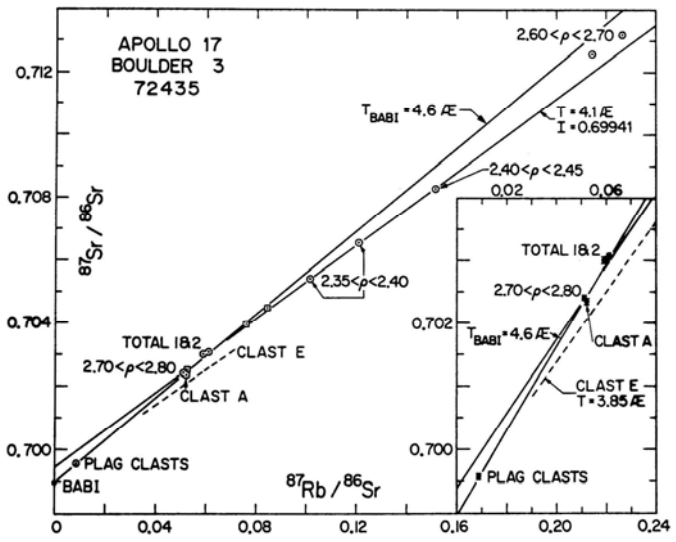

Figure 12: Rb-Sr evolution diagram for materials from 72435 (Papanastassiou and Wasserburg, 1975a). All ages on the diagram are for the old decay constant of 1.39 x j o-11 [3-1.] Lack of isotopic homogenization at any unique time in the past is obvious (a) for total rocks and clasts and (b) for mineral separates from the finer-grained matrix. The dashed line is for interior samples from clast E.

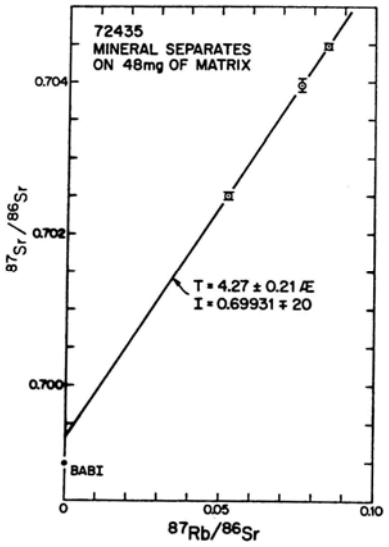

Figure 13. Rb-Sr evolution diagram for mineral separates from a 48 mg matrix sample of 72435 (Papanastassiou and Wasserburg, 1975a). The it of the data to a straight line could result from mixing of only two phases. The age is for the old decay constant of 1.39 x 10-11 y-1

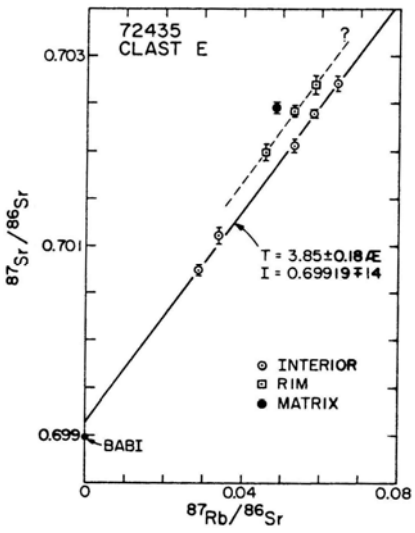

Figure 14: Rb-Sr evolution diagram for clast E from 72435 (Papanastassiou and Wasserburg, 1975a). Interior samples define a straight line (solid) from which rim and adjacent matrix samples are offset. The age (given on the diagram for the old decay constant of 1.39 x 10-11 [y-1)] has a large uncertainty because of the low spread in Rb/Sr.

the matrix and clasts do not fall on an isochron (Fig. 12); the plagioclases on a whole-rock-$_{TBABI}$ line equivalent to 4.5 Ga. Thus there is no Sr isotopic equilibration between matrix and clasts. (However, the paper refers to a Pb isotope study by Tera and Wasserburg that shows Pb equilibration between matrix and plagioclase clasts in 72435 at about 3.8 Ga; the reference given is erroneous). The density separates on the matrix also do not he on a straight line so the matrix is not homogeneous. Matrix separates for a single 48 mg split fall on a line corresponding to an age of 4.18 +/- 0.21 Ga (Fig. 13) but little credence can be given to such an age with the data available, the small spread in Rb/Sr, and the independent data for a younger age for the matrix-forming event. Data for clast E (predominantly plagioclase with a range of compositions) are shown in Figs. 14 and 15, with clast interior, rim, and adjacent matrix shown separately. The clast data correspond with an age of 3.77 +/- 0.18 Ga; with large uncertainties resulting from the small spread in Rb/Sr. The adjacent rim and matrix samples fall distinctly off the isochron. Papanastassiou and Wasserburg (1975a) could not distinguish whether the age of the clast was primary or metamorphic. The lowest model ages for breccia components are those of separates of clast E at about 3.9 Ga (decay constant 1.42 x 10^{-11} $Y^{-1)}$, and these are maximum ages for breccia formation. The age of clast E itself would indicate a younger age or some disturbance.

Huneke et al. (1977) reported argon isotopic data for 4 combined plagioclase clasts from 72435, totaling 1.5 mg with 530 ppm K. The age is constant at 3.87 +/- 0.07 (new constant) over the entire release (Fig. 16), with no suggestion of older ages suggested by the primitive Sr isotopes in 72435 plagioclases. Huneke and Wasserburg (1978) and Huneke (1978) reported further studies on

argon isotopes in two individual clasts (Fig. 17), tabulating release data. One consisting of a plagioclase crystal and 25% matrix (0.4 mg; 1200 ppm K) gave a well-defined age of 3.86 +/- 0.04 Ga over the entire release. A large plagioclase crystal (0.6 mg; 190 ppm K) gave a similar age over the first 40% of ^{39}Ar release, then the age rose to 4.04 Ga for the remainder of the release. This plagioclase was incompletely degassed at 3.86 Ga, and 4.04 Ga is a lower limit to its age.

Goswami et al (1976a) reported track data for 72435. The boundary-track method gave preliminary results of an upper limit to compaction less than 4.1 Ga ago. A more precise determination was hindered by a lack of cosmic ray exposure ages, as there was a high background of cosmic ray tracks. No data were presented

PHYSICAL PROPERTIES

Pearce et al (1974a,b) listed the magnetic properties of 72435,1 (Table 6) without specific discussion. The metallic iron contents are similar to other Apollo 17 impact melts and much higher than mare basalts. The metal is coarse-grained with low J_{rs}/J_s.

PROCESSING

The sample was received as two pieces originally numbered as 72435 and 72436; they were combined as 72335 when it was realized that they fitted together. Two small chips (,1; ,2) were removed from ,0. Advantage was taken of the natural break to produce a slab across the sample with only one saw cut, leaving the large E end ,13 (now 71 g), the W end ,22 (two broken pieces, 40 g, now at Brooks), and the slab sections (Fig. 2). The slab was subdivided by perpendicular saw cuts and most allocations from it. One piece, 11(21 g) was sent for subdivision and study by the consortium led from Caltech. Some matrix pieces were taken from ,22 before it was stored at Brooks

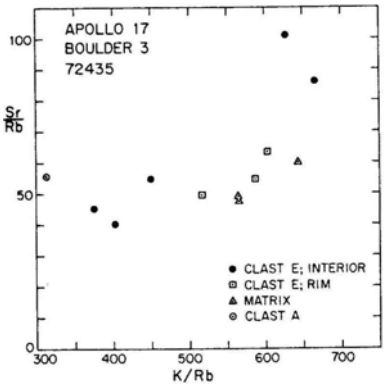

Figure 15. Element correlation diagram for samples from 72435 (Papanastassiou and Wasserburg, 1975a). Samples of clast E require the presence of at least 3 phases; the matrix and clast E rim appear distinct from clast E.

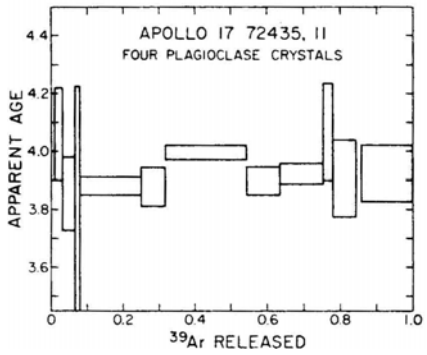

Figure 16: Apparent age of four combined plagioclases from 72435 (Huneke et al., 1977). Age scale is for old decay constants

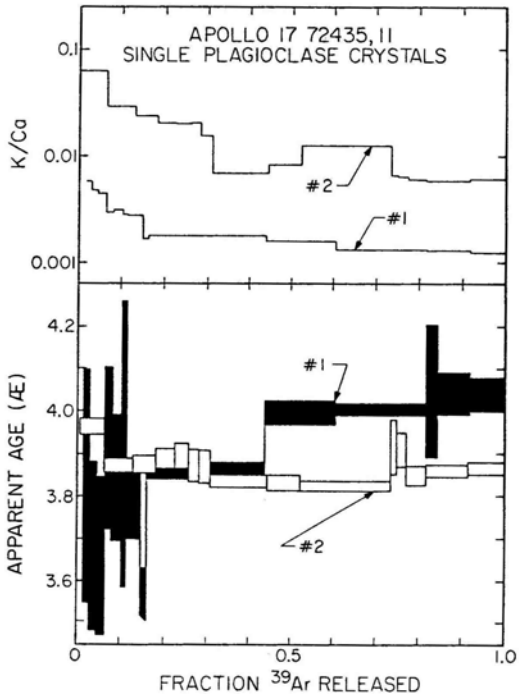

Figure 17: Apparent age of clasts from 72435 (Huneke, 1978). Clast 1 is plagioclase; Clast 2 is plagioclase + 25% matrix. Age scale is for new decay constants.

Table 6: Magnetic properties of 72435, 1. Pearce et al (1974a, b)

Sample	J_s (emu/g)	X_p (emu/g Oe) $\times 10^6$	X_0 (emu/g Oe) $\times 10^4$	J_{rs}/J_s	H_c (Oe)	H_{cr} (Oe)	Equiv. wt.% Fe^0	Equiv. wt.% Fe^{++}	$\frac{Fe^0}{Fe^{++}}$
72435,1	.86	14.9	2.1	.003	19	—	.39	6.83	.058